JOURNAL OF MATERIALS SCIENCE 23 (1988) 982–986

Microstructural development of a ZrO_2–Naβ''-Al_2O_3 composite

YIN SHENG, PATRICK S. NICHOLSON
Ceramic Engineering Research Group, Department of Materials Science and Engineering, McMaster University, Hamilton, Ontario, Canada

Microstructural development in Naβ''-Al_2O_3 containing 15 vol % ZrO_2 particles is described. Intergranular ZrO_2 particles inhibit abnormal grain growth of the Naβ''-Al_2O_3. The growth of the Naβ''-Al_2O_3 grains and the intergranular ZrO_2 followed a cubic time law. Direct particle coalescence consisting of encounter and spheroidizing processes was found to be the basic growth mechanism for the intergranular ZrO_2.

1. Introduction

ZrO_2 transformation-toughened ceramics require that tetragonal ZrO_2 be retained at room temperature. The retention of tetragonal ZrO_2 depends on the ZrO_2 particle size, i.e. a critical particle size exists below which the tetragonal-to-monoclinic ZrO_2 transformation does not occur. It is therefore important to understand how to control the ZrO_2 particle size in zirconia-containing composites. In this work, the growth process in ZrO_2–Naβ''-Al_2O_3 composites was studied. Second-phase particle growth is usually attributed to diffusion or interface-controlled Ostwald ripening [1, 2]. In most systems the measured particle size distribution is much broader than predicted by classical diffusion-controlled Ostwald ripening theory. Recently a direct particle-coalescence theory has been developed [3, 4] which may explain this discrepancy. Two ZrO_2 morphologies exist in ZrO_2–Naβ''-Al_2O_3 composites, i.e. intergranular and intragranular ZrO_2 particles. Transformation toughening is usually attributed to the intergranular ZrO_2. This paper discusses the particle growth mechanism of the intergranular ZrO_2 in 15 vol % ZrO_2–Naβ''-Al_2O_3 composites.

Large grains within a fine-grain matrix are usually the fracture origins. A duplex microstructure is often the reason that Naβ''-Al_2O_3 ceramics are weak. ZrO_2 particles limit abnormal grain growth in Naβ''-Al_2O_3 and so improve the mechanical properties [5].

2. Experimental procedure

15 vol % ZrO_2–Naβ''-Al_2O_3 composites were prepared by conventional methods using the powder route described as Route II in a companion paper [5]. Large ZrO_2–4.5 wt % Y_2O_3 agglomerates were first removed from the ZrO_2 powder by sedimentation in water. The ZrO_2 powders, Na_2CO_3, MgO and Al_2O_3 were then mixed and milled in ethanol for 48 h, dried and calcined 5 h at 1000° C. The sieved composite powders were uniaxially pressed, isostatically pressed and sintered at 1620° C. To compare the microstructural development of the ZrO_2–Naβ''-Al_2O_3 composites with that of single-phase Naβ''-Al_2O_3 and single-phase ZrO_2, the three materials were sintered under the same sintering conditions. Sintered samples were polished, thermally etched, and examined by SEM. The Naβ''-Al_2O_3 grain size and the ZrO_2 particle size distribution were measured using an image analyser. The experimental particle size distributions were normalized in order to identify the particle growth mechanism [6].

3. Results and discussion

Typical micrographs of single-phase Naβ''-Al_2O_3 and 15 vol % ZrO_2–Naβ''-Al_2O_3 composites are shown in Figs 1 and 2, respectively. Table I lists the mean ZrO_2 grain size for single-phase ZrO_2, the mean Naβ''-Al_2O_3 grain size for single-phase Naβ''-Al_2O_3, and the mean particle size of ZrO_2 and the mean Naβ''-Al_2O_3 grain size for the 15 vol % ZrO_2–Naβ''-Al_2O_3 composites sintered at 1620° C for 5, 25, 60 and 120 min.

The microstructures obtained for single-phase Naβ''-Al_2O_3 are similar to those reported for other Naβ/β''-Al_2O_3 materials. Figs 1a and b show the uniform fine-grained microstructure which develops after short sintering times. Figs 1c and d illustrate the occurrence of secondary recrystallization with longer sintering times. Abnormal grain growth and the typical duplex microstructure began to appear after sintering for 30 min, i.e. a few larger lath-shaped grains embedded in a fine-grained matrix.

Comparing the microstructures of single-phase Naβ''-Al_2O_3 and those of the 15 vol % ZrO_2–Naβ''-Al_2O_3 composite illustrates the ZrO_2-controlled microstructural differences. For short-time-sintered Naβ''-Al_2O_3, most of the grains were rod-shaped. The

TABLE I Mean grain (particle) size for different sintering times

Materials	Mean grain size (μm)			
	5 min	25 min	60 min	120 min
Single-phase ZrO_2	0.39	0.58	0.75	0.94
Single-phase Naβ''-Al_2O_3	0.61	0.81	1.2	1.54
ZrO_2–Naβ''-Al_2O_3 composite				
ZrO_2 particles	0.55	0.57	1.03	1.43
β''-Al_2O_3 grains	0.49	0.89	1.59	2.06

0022–2461/88 $03.00 + .12

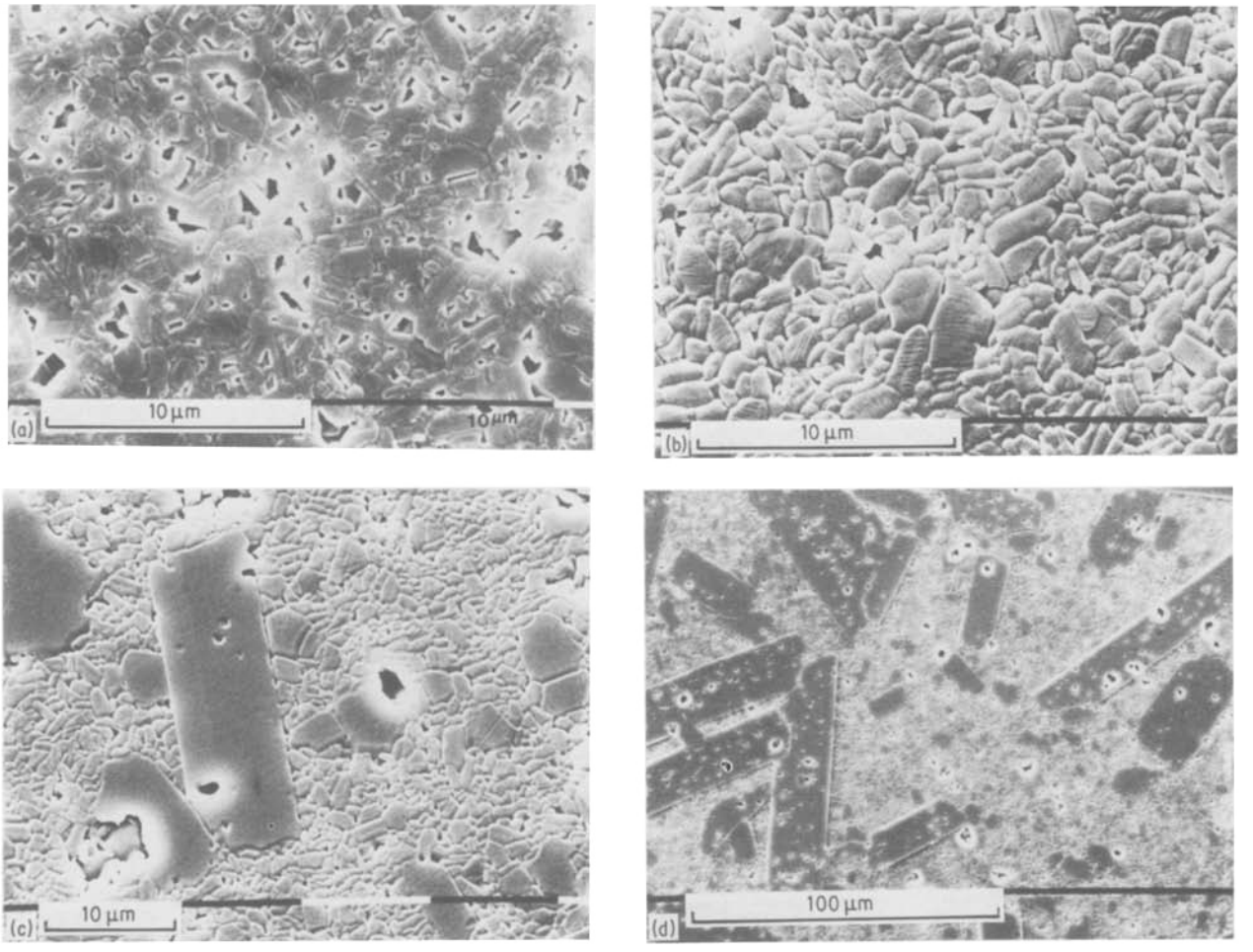

Figure 1 SEM micrographs of single-phase Naβ''-Al_2O_3 sintered at 1620° C for (a) 5 min, (b) 25 min, (c) 60 min, (d) 120 min.

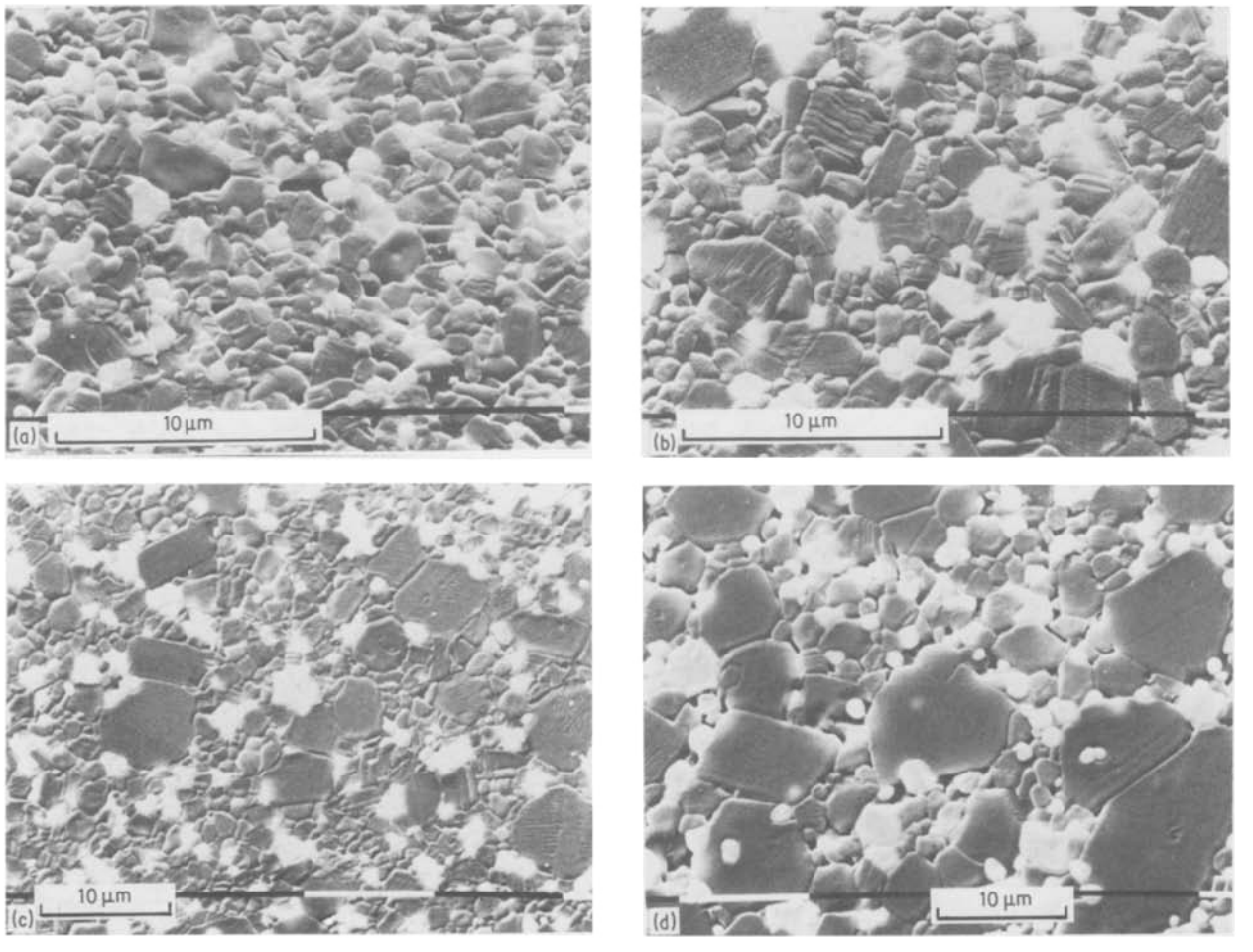

Figure 2 SEM micrographs of 15 vol % ZrO_2–Naβ''-Al_2O_3 sintered at 1620° C for (a) 5 min, (b) 25 min, (c) 60 min, (d) 120 min.

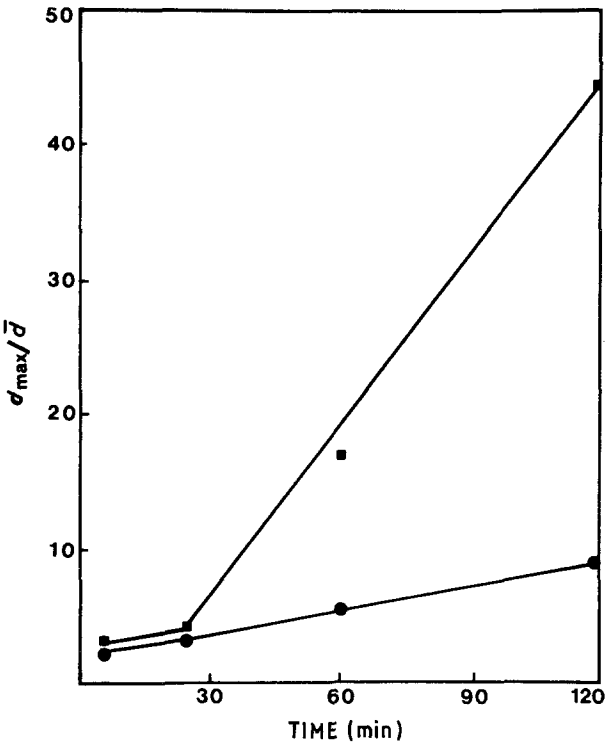

Figure 3 The ratio of largest to mean grain size of β''-Al_2O_3 against sintering time in single-phase Naβ''-Al_2O_3 and in ZrO_2–Naβ''-Al_2O_3: (■) single-phase β''-Al_2O_3, (●) ZrO_2–Naβ''-Al_2O_3.

Naβ''-Al_2O_3 phase had a polyhedral grain shape in the ZrO_2–Naβ''-Al_2O_3 composite. During sintering, the ZrO_2 particles inhibit the preferred-orientation grain growth characteristic of the Naβ''-Al_2O_3 and shape changes caused by shape accommodation. In the 60 min sintered Naβ''-Al_2O_3, the largest grain size was $\sim 20\,\mu m$ and the large lath-shaped grains had an aspect ratio of $\sim 5:1$. In the ZrO_2–Naβ''-Al_2O_3 composites, the largest Naβ''-Al_2O_3 grain size was $9\,\mu m$ and the aspect ratio was $< 2:1$. Fig. 3 is a plot of the ratio of largest Naβ''-Al_2O_3 grain size (d_{max}) to the mean grain size (d) as a function of sintering time for

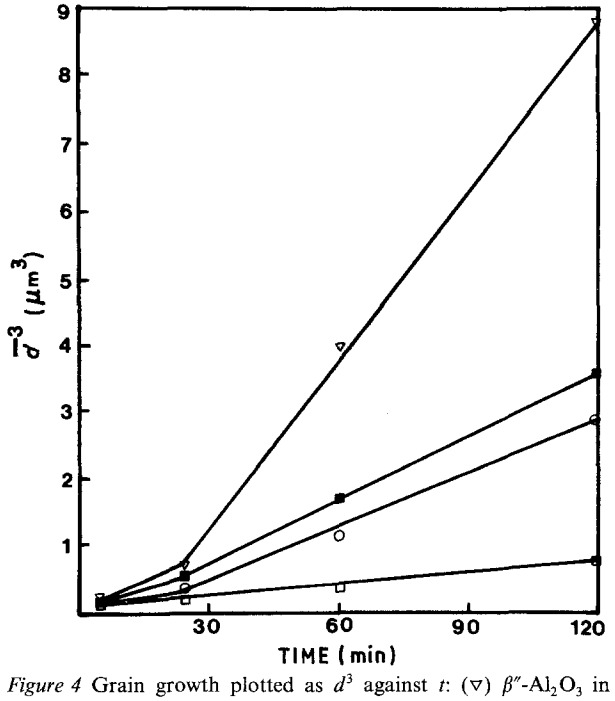

Figure 4 Grain growth plotted as d^3 against t: (▽) β''-Al_2O_3 in ZrO_2–Naβ''-Al_2O_3; (■) single-phase β''-Al_2O_3; (○) ZrO_2 particles in ZrO_2–Naβ''-Al_2O_3; (□) single-phase ZrO_2.

both materials. This figure clearly illustrates the role of the ZrO_2 particles in limiting the abnormal grain growth of the Naβ''-Al_2O_3 phase. The Naβ''-Al_2O_3 grain size and the proportion of large grains increases with increasing sintering time in both materials. The experimentally observed grain growth kinetics of the Naβ''-Al_2O_3 phase in both systems is described by a cubic time law, i.e.

$$\bar{d}^3 = kt \tag{1}$$

where $\bar{d}$ is the mean grain size of the Naβ''-Al_2O_3 and t is the sintering time.

The grain growth of single-phase ZrO_2 and the intergranular ZrO_2 particle growth in the 15 vol % ZrO_2–Naβ''-Al_2O_3 also follow the cubic time law (Fig. 4). Second-phase particles in two-phase alloys or two-phase ceramics can grow by Ostwald ripening and/or by a coalescence mechanism. In the Ostwald ripening theory, the mean particle size is proportional to the cube root of time. In the coalescence theory of particle growth, the particle size also obeys the cubic time law. Davies *et al.* [3] observed second-phase particle "encounter" in ageing alloys and derived the equation

$$\bar{R}^3 - \bar{R}_0^3 = \frac{6\sigma V_m C_e D \bar{r}^3}{RT\gamma} t \tag{2}$$

where $\bar{R}$ and $\bar{R}_0$ are the initial mean radii and actual mean particle radii, σ is the surface energy of the particle–matrix interface, V_m the molar volume of the particle, C_e the mole fraction of solute in matrix at equilibrium, D the diffusion coefficient, t the time, RT has its usual meaning, $\bar{r}^3 = (\bar{R}/\bar{R}_c)^3$ where $\bar{R}_c$ is the critical radius, and $\gamma = 3dt'/dx^3$; t' is a dimensionless quantity proportional to real time t and $x = \bar{R}_c/\bar{R}_{co}$, where $\bar{R}_{co}$ is the critical radius at the onset of coarsening. This equation is similar to the Lifshitz–Slyozov–Wagner (LSW) equation of Ostwald ripening theory [1, 2].

In the coalescence theory of Takazo *et al.* [4], second-phase particle coalescence in a liquid-phase-sintering system was treated by a statistical approach assuming that direct particle coalescence was the basic growth mechanism. This theory also suggests that the increase of average particle size is proportional to the cube root of sintering time and a basic equation describing the particle size distribution during sintering was derived.

The particle size distributions obtained via the Ostwald ripening and the coalescence mechanisms are different. In the LSW Ostwald ripening theory, the range of particle size obtained is narrow and the particle size distribution is skewed toward finer particles. It also predicts a sharp "cut-off" at $1.5\bar{d}$.

The LSW theory is strictly only applicable when the volume fraction of particles tends towards zero (Fig. 5, Line 1). Modified Ostwald ripening theories [6, 7] which take the effect of larger volume fractions into account give broader particle size distributions and provide better agreement with experimental results (Fig. 5, Line 2). In some systems, however, the measured particle size distribution is broader than these predicted curves. The particle size distribution

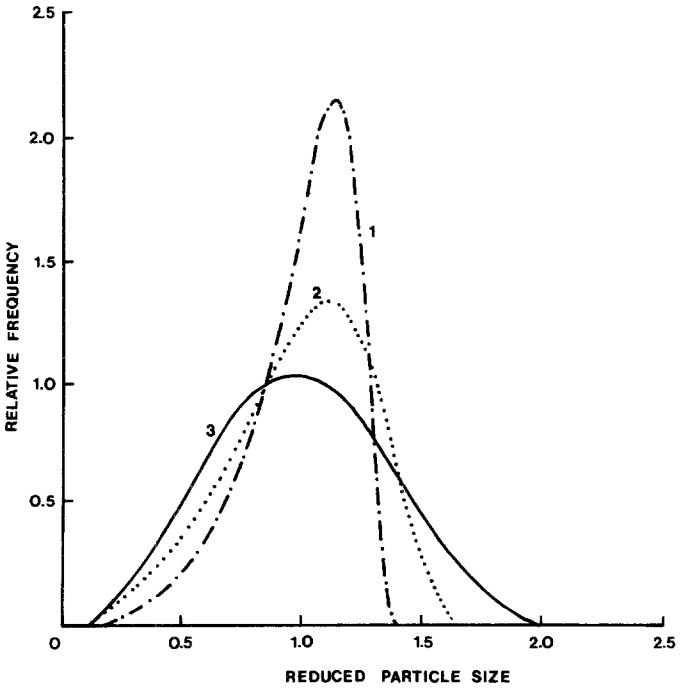

Figure 5 Normalized particle size distribution calculated on the basis of coalescence (——) and on the basis of Ostwald ripening (—·—·—) volume fraction = 0.2, (····) volume fraction = 0.8 [4].

calculated when direct particle coalescence occurs is much broader, possesses no "cut-off" particle size and shows an exponential decrease for large particle sizes (Fig. 5, Line 3) [4].

The normalized particle size distribution of intergranular ZrO_2 in the 15 vol % ZrO_2–Naβ''-Al_2O_3 composites is shown in Fig. 6. Taken in conjunction with the microstructural observations, Fig. 6 suggests that direct particle coalescence is the basic growth mechanism of intergranular ZrO_2 in these composites. Ostwald ripening also contributes to the ZrO_2 particle growth as shown later. The coalescence of intergranular ZrO_2 particles involves two processes, i.e., "encounter" and spheroidization.

The encounter process can proceed in two ways. When a particle is growing by Ostwald ripening, its boundary expands outwards until it touches another particle (Fig. 7a). An alternative mechanism of encounter involves grain growth of the matrix grains with the concomitant disappearance of small matrix grains. This process also causes the intergranular second-phase particles to meet [8] (Fig. 7b). These two processes usually occur simultaneously. Another point in the ZrO_2–Naβ''-Al_2O_3 composites is that many of the ZrO_2 particles are probably agglomerated in the original matrix powder.

The spheroidization of particles describes the morphological change process of the encountered particles. Two types of morphology are possible. In the case of the particle couple consisting of a large particle and a small one, "engulfment" of the small particle by the larger one will occur by Ostwald ripening [9] (Fig. 8a). For a particle couple consisting of equisized particles, the mode of morphological change could be characterized by a gradual increase in the ratio of the weld size to the particle size (Fig. 8b). The morphological change of the ZrO_2 agglomerates is shown in Fig. 8c and was observed to occur with increasing sintering time. After sintering for 2 h, most of the ZrO_2 particles are spheroidal (Fig. 2d). For short sintering

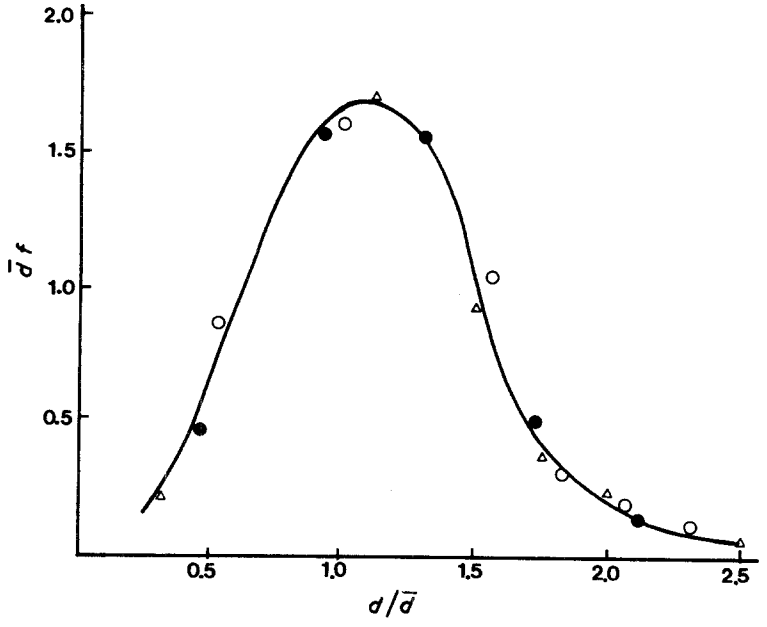

Figure 6 Normalized particle size distribution of intergranular ZrO_2 in 15 vol % ZrO_2–Naβ''-Al_2O_3 (f = frequency). Sintering time (●) 5 min, (○) 60 min, (△) 120 min.

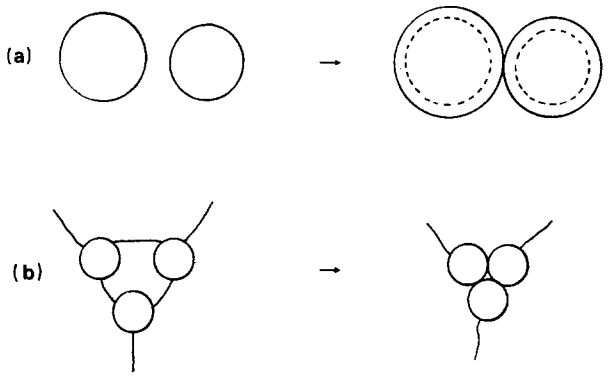

Figure 7 (a, b) Intergranular ZrO_2 particle encounters.

times, some of the particles were irregular and weld boundaries could be seen.

In the 15 vol % ZrO_2–Naβ''-Al_2O_3 composites, the majority of ZrO_2 particles were intergranular; however, some intragranular ZrO_2 was observed. The distribution of this intragranular ZrO_2 within the Naβ''-Al_2O_3 was inhomogeneous (Fig. 9). During the grain growth process some Naβ''-Al_2O_3 grains have entrapped some initial intergranular ZrO_2. These intragranular ZrO_2 particles are much larger than the original intragranular ZrO_2. The kinetics of particle growth of the intragranular ZrO_2 did not follow any consistent time law. This finding agrees with that of Kibbel and Heller [8].

4. Conclusions

The ZrO_2 particles in 15 vol % ZrO_2–Naβ''-Al_2O_3 composites are primarily intergranular but some intragranular ZrO_2 was observed. The intergranular ZrO_2 particles inhibit abnormal growth of the Naβ''-Al_2O_3 grains. The Naβ''-Al_2O_3 grains developed polyhedral morphology by shape accommodation instead of the characteristic lath-shape grains observed in single-phase Naβ''-Al_2O_3. The increase of the mean Naβ''-Al_2O_3 grain size and the mean intergranular ZrO_2 particle size followed a cubic time law. Direct particle coalescence was identified as the major growth mechanism but Ostwald ripening was observed to contribute. The coalescence of the intergranular ZrO_2 particles progressed via encounter and spheroidization processes. The intragranular ZrO_2 particles were inhomogeneously distributed.

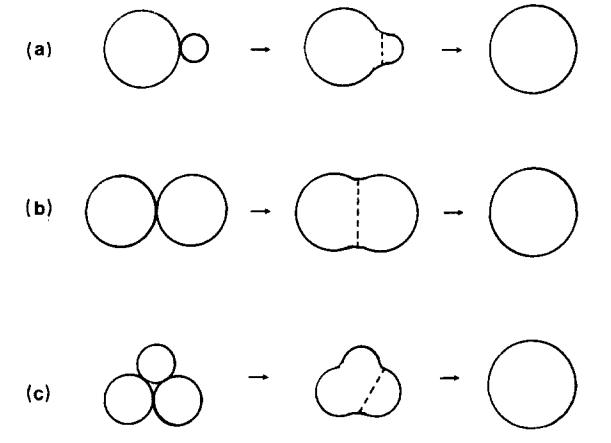

Figure 8 (a–c) Particle spheroidization.

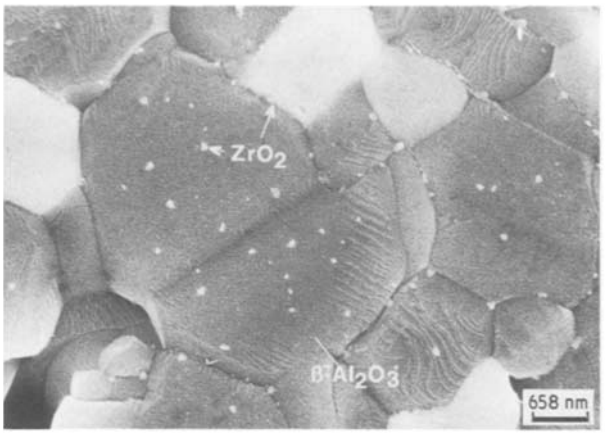

Figure 9 Intragranular ZrO_2 particles in 15 vol % ZrO_2–Naβ''-Al_2O_3.

References

1. I. M. LIFSHITZ and V. V. SLYOZEV, *J. Phys. Chem. Solids* **19** (1961) 35.
2. C. WAGNER, *Z. Elektrochem.* **65** (1961) 581.
3. C. K. L. DAVIES, P. NASH and R. N. STEVENS, *Acta Metall.* **28** (1980) 179.
4. S. TAKAZO, W. A. KAYSSER and G. PETZOW, *ibid.* **32** (1984) 107.
5. YIN SHENG and P. S. NICHOLSON, *J. Mater. Sci.* **23** (1988) 958.
6. A. J. ARDELL and R. B. NICHOLSON, *J. Phys. Chem. Solids* **27** (1966) 1793.
7. A. D. BRAILSFORD and P. WYNBLATT, *Acta Metall.* **27** (1979) 489.
8. B. W. KIBBEL and A. H. HELLER, *Adv. Ceram.* **12** (1984) 415.
9. K. WATANABLE and Y. MASUDA, in "Sintering and Catalysis," edited by G. C. Kuczynski, International Conference on Sintering and Related Phenomena (Plenum Press, New York, 1975) p. 389.

Received 28 April
and accepted 6 July 1987